






Article

Moesin (*MSN*) as a Novel Proteome-Based Diagnostic Marker for Early Detection of Invasive Bladder Urothelial Carcinoma in Liquid-Based Cytology

Jeong Hwan Park ^{1,2,†} , Cheol Lee ^{1,3,†} , Dohyun Han ^{4,5,†} , Jae Seok Lee ^{6,†}, Kyung Min Lee ⁷, Min Ji Song ³, Kwangsoo Kim ⁴ , Heonyi Lee ^{4,5}, Kyung Chul Moon ^{1,3}, Youngsoo Kim ⁸, Minsun Jung ^{1,3} , Ji Hye Moon ^{1,3}, Hyebin Lee ^{9,*} and Han Suk Ryu ^{1,3,*}

¹ Department of Pathology, Seoul National University College of Medicine, Seoul 03080, Korea; hopemd@hanmail.net (J.H.P.); fejh@hanmail.net (C.L.); blue7270@gmail.com (K.C.M.); jjunglammy@gmail.com (M.J.); sssince2004@naver.com (J.H.M.)

² Department of Pathology, SMG-SNU Boramae Medical Center, Seoul 07061, Korea

³ Department of Pathology, Seoul National University Hospital, Seoul 03080, Korea; minji891111@nate.com

⁴ Division of Clinical Bioinformatics, Biomedical Research Institute, Seoul National University Hospital, Seoul 03080, Korea; hdh03@snu.ac.kr (D.H.); kksoo716@gmail.com (K.K.); hylee4161@gmail.com (H.L.)

⁵ Proteomics Core Facility, Biomedical Research Institute, Seoul National University Hospital, Seoul 03080, Korea

⁶ Department of Pathology, Samsung Changwon Hospital, Sungkyunkwan University School of Medicine, Changwon 51353, Korea; hymedljs@naver.com

⁷ Center for Medical Innovation, Biomedical Research Institute, Seoul National University Hospital, Seoul 03082, Korea; km601@naver.com

⁸ Department of Biomedical Sciences, Seoul National University College of Medicine, Seoul 03080, Korea; biolab@snu.ac.kr

⁹ Department of Radiation Oncology, Kangbuk Samsung Hospital, Sungkyunkwan University School of Medicine, Seoul, 03181, Korea

* Correspondence: hyebin.lee@samsung.com (H.L.); nash77@snu.ac.kr (H.S.R.)

† These authors contributed equally to this work.

Received: 20 March 2020; Accepted: 16 April 2020; Published: 21 April 2020



Abstract: Bladder urothelial carcinoma (BUC) is the most lethal malignancy of the urinary tract. Treatment for the disease highly depends on the invasiveness of cancer cells. Therefore, a predictive biomarker needs to be identified for invasive BUC. In this study, we employed proteomics methods on urine liquid-based cytology (LBC) samples and a BUC cell line library to determine a novel predictive biomarker for invasive BUC. Furthermore, an in vitro three-dimensional (3D) invasion study for biological significance and diagnostic validation through immunocytochemistry (ICC) were also performed. The proteomic analysis suggested moesin (*MSN*) as a potential biomarker to predict the invasiveness of BUC. The in vitro 3D invasion study showed that inhibition of *MSN* significantly decreased invasiveness in BUC cell lines. Further validation using ICC ultimately confirmed moesin (*MSN*) as a potential biomarker to predict the invasiveness of BUC ($p = 0.023$). In conclusion, we suggest moesin as a potential diagnostic marker for early detection of BUC with invasion in LBC and as a potential therapeutic target.

Keywords: bladder urothelial carcinoma; invasion; biomarker; proteomics; liquid-based cytology; moesin

1. Introduction

Bladder urothelial carcinoma (BUC) is the most common and lethal malignancy of the urinary tract [1]. The evaluation of cancer cell invasion beyond the subepithelial layer is crucial due to the

availability of different therapeutic approaches [2], which has prompted the identification of robust invasion-associated molecular characteristics of BUC [3,4].

Unlike extensive genome-based studies, in-depth proteomic analysis of BUC has been introduced in a few studies [5–10], among which only one study identified predictive markers for tumor invasion in muscle-invasive BUC (MIBUC) by predominantly using human-derived tissue samples and proteomic approaches [7].

In our previous study, we successfully conducted a proteomic study and validated a proteome-based novel diagnostic marker of BUC in liquid-based cytology (LBC) [11], which is the gold standard test for surveillance of urothelial carcinoma recurrence or progression [12,13]. Voided urine cytology used in this study is the standard non-invasive method for the detection of BUC by the assessment of morphologic changes of exfoliated urothelial cells in comparison to transurethral endoscopy which is more invasive and expensive. Recent cytologic slide-based ancillary tests showed anticipatory positive results by direct integration with cytomorphologic findings [14].

Moesin is a protein encoded by the *MSN* gene at chromosome location Xq12 as a member of the ERM (ezrin, radixin, and moesin) family [15,16] and is known to be associated with an aggressive phenotype in several malignant tumors [16–19]. Higher *MSN* mRNA expression was also significantly associated with unfavorable survival in various types of human cancers, including lung, stomach, and pancreatic cancer in The Cancer Genome Atlas (TCGA) dataset [20].

In this study, we explored proteome-based novel biomarkers to predict advanced tumor stage in voided urine cytology samples collected by liquid-based preparation and evaluated the predictive ability of moesin (*MSN*) in the context of BUC invasion through immunocytochemistry (ICC) validation in independent LBC cohorts. Finally, we investigated its functional role in cancer invasion with a three-dimensional (3D) in vitro invasion assay.

2. Results

2.1. Proteomic Analysis Identified Cancer Invasion-Associated Protein Groups in Urine Liquid-Based Cytology

In total, 3259 and 1779 proteins were identified and quantified at the 1% false discovery rate (FDR) level by a single-shot proteomic analysis of the LBC samples (Table S1). For each case, the average number of identified and quantified proteins was demonstrated in Figure S1. Multigroup tests with one-way ANOVA revealed 182 differentially expressed proteins (DEPs) among three cohorts based on pathologic T (pT) stage (Figure 1A, Table S2). The hierarchical clustering was classified into four groups based on the proteome expression (Figure 1A). The protein expression of *KPNA3* [21], *TACSTD2* [22], *GRHL2* [23], *NCAM2* [24], *LLGL2* [25], *ATP1B1* [26], *CLTC* [27], *PARP4* [28], *MVP* [29], and *PPA2* [20] that play a tumor-suppressive role was increased in non-invasive BUC (NIBUC) compared to invasive BUC (Group 1). On the other hand, several proteins promoting cell motility and invasion, including *ARHGEF2* [30], *MSN* [16,18,19], *VIM* [31], *LCPI* [32], *FLNA* [33], *FERMT3* [34], *ITGAM* [35], and *CORO1A* [36] were significantly upregulated in MIBUC (Group 3, Figure 1A). A further two-group analysis between NIBUC and MIBUC also demonstrated the overexpression of DEPs with a tumor-suppressive role, including *LGALS3* [37] and *VAPA* [21] in NIBUC (Figure 1B, Table S3). Several key proteins such as *MAP2K1* [38], *ITGB4* [39], *ITGA6* [40], *PTPN6* [41], *FMNL1* [42], *ANXA1* [43], and *MMP9* [44] that modulate cell motility and tumor cell invasion were upregulated in MIBUC (Figure 1B, Table S3). Together, our proteomic findings suggested a cooperative interaction among several genes in the invasive process of BUC.

Subsequently, a gene ontology analysis on biological process revealed enrichment in cytoskeleton organization, cell migration, and cell motility, which implicated significant alterations in the cytoskeletal architecture and invasion process (Figure 1C, Table S4). Especially, DEPs involved in cell motility and invasion were mostly upregulated in MIBUC compared to NIBUC. A further comparison of stromal-invasive BUC (SIBUC) and NIBUC revealed that biological processes with ribonucleoprotein complex biogenesis and antigen processing/presentation of peptide antigen were significantly enriched

in SIBUC by upregulated and downregulated DEPs, respectively (Figure S2, Table S4–S6). Molecular functions with UFM1 activating enzyme activity and oxidoreductase activity were enriched while comparing MIBUC and SIBUC groups.

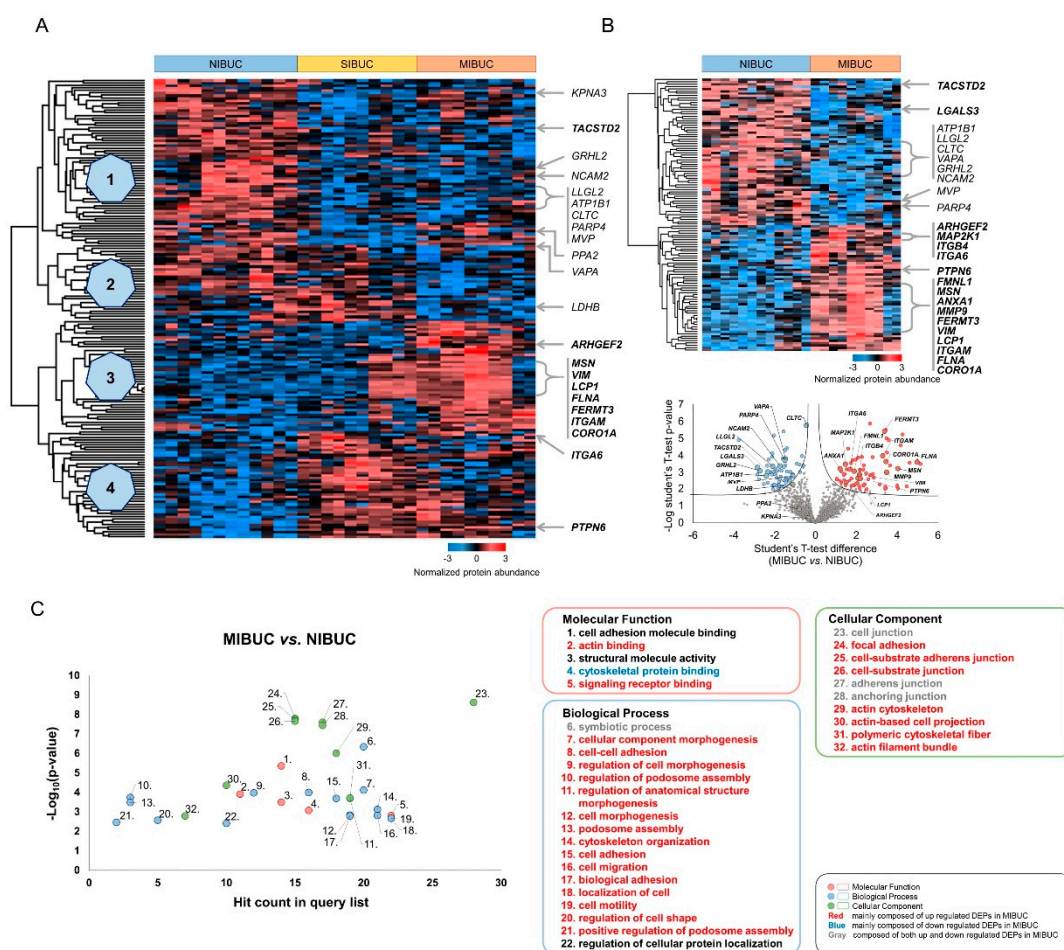


Figure 1. Results of proteomic analysis of bladder urothelial carcinoma (BUC) in liquid-based cytology (LBC) samples. (A) Hierarchical clustering of 16 BUC LBC proteomic data among non-invasive BUC (NIBUC), stromal-invasive BUC (SIBUC), and muscle-invasive BUC (MIBUC) (Group 1, downregulated in invasive BUC; Group 2, downregulated in MIBUC; Group 3, upregulated in MIBUC; Group 4, upregulated in invasive BUC). (B) Hierarchical clustering and volcano plot between MIBUC and NIBUC. (C) Gene ontology results between MIBUC and NIBUC.

2.2. Proteomic Library of BUC Cell Lines Identified Candidate Biomarkers

For the discovery of candidate biomarkers related to invasion, we performed a tandem mass tag (TMT) proteomic analysis and constructed a BUC cell line proteomic library (Figure 2, Table S7). First, we assessed the invasion and migration ability of eight BUC cell lines to categorize them into invasive BUC cell line (IBUC_CL) and non-invasive BUC cell line (NIBUC_CL). Among the BUC cell lines, T24, J82, and 253J-BV (IBUC_CL) revealed the most invasive and proliferative capacity, while RT4, HT1376, and HT1197 showed the least aggressive ability (NIBUC_CL) (Figure 2A,B). Next, we conducted a proteomic analysis between IBUC_CL and NIBUC_CL for the discovery of candidate biomarkers related to cancer invasion and identified 677 DEPs and aforementioned proteins in LBC proteomics, including *ATP1B1*, *CLTC*, *GRHL2*, *KPNA3*, *LDHB*, *LLGL2*, *MSN*, *MVP*, *NCAM2*, *PARP4*, *PPA2*, and *VAPA* (Figure 2C, Table S8).

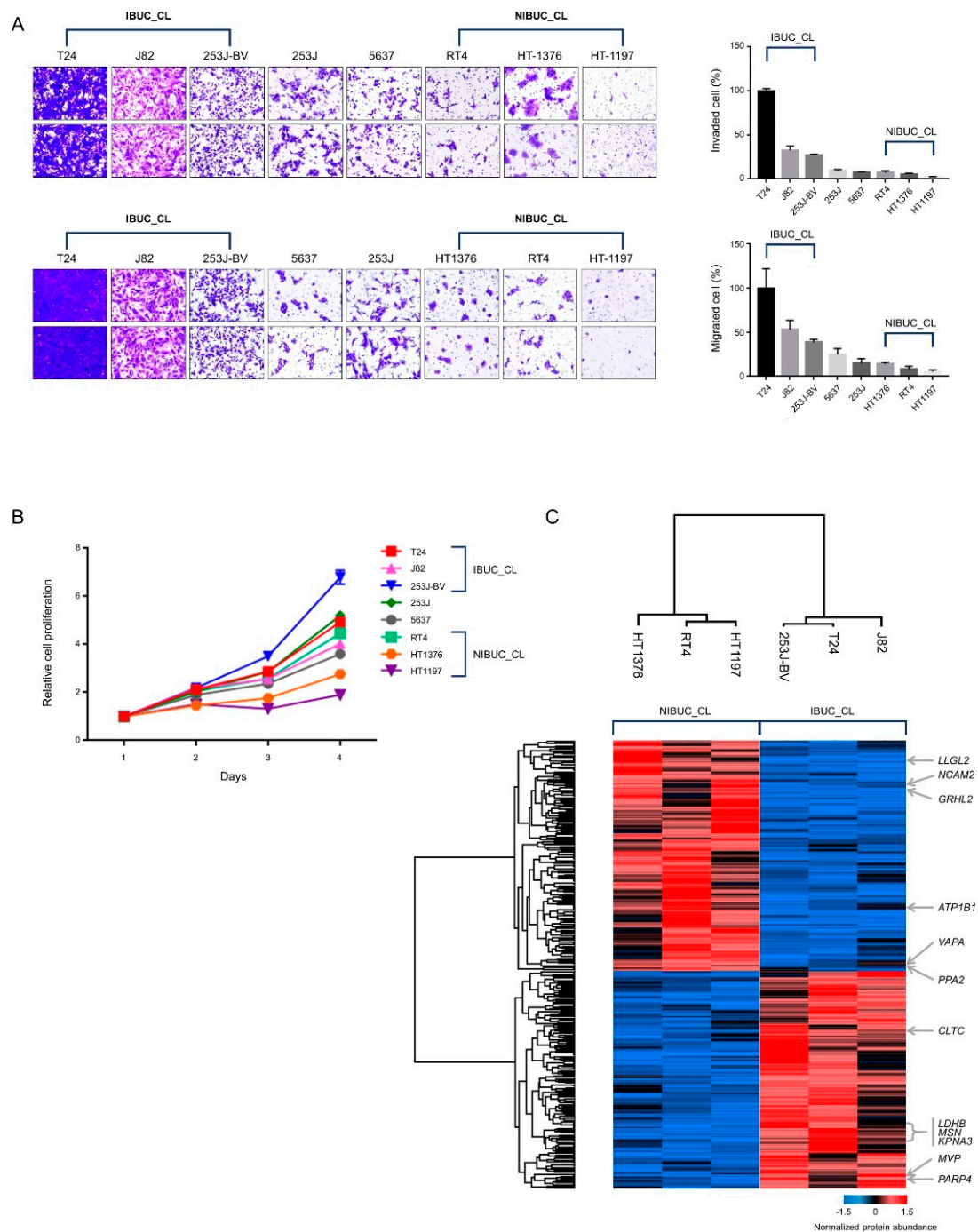


Figure 2. Bladder urothelial carcinoma (BUC) cell line results. **(A)** Invasion and migration Assay. **(B)** Proliferation assay. **(C)** Hierarchical clustering of differentially expressed proteins (DEPs) between invasive bladder urothelial carcinoma cell line (IBUC_CL) and non-invasive bladder urothelial carcinoma cell line (NIBUC_CL).

2.3. Multi-Omic Platforms Selected Moesin (MSN) as a Potential Biomarker for Invasive BUC

For the discovery of potential biomarkers related to invasion, we performed a stepwise analysis on a multilayer platform (Figure 3A, Table S9). First, we compared DEPs from one-way ANOVA and paired t-test of LBC samples. Proteomic analysis of LBC revealed 182 DEPs and 188 DEPs in one-way ANOVA and paired t-test, respectively. Cross-validation with these two platforms showed 139 common DEPs in LBC proteomics. Next, we employed an extra platform of BUC cell line proteomics to determine a predictive biomarker for bladder cancer invasion. We used the 677 proteins for BUC cell line

proteomics for a comparative analysis with DEPs derived from human LBC proteomics. Consequently, the cross-validation of DEPs from LBC and BUC cell lines revealed 12 invasion-associated biomarker candidates: *ATP1B1*, *CLTC*, *GRHL2*, *KPNA3*, *LDHB*, *LLGL2*, *MSN*, *MVP*, *NCAM2*, *PARP4*, *PPA2*, and *VAPA*.

To shortlist the optimal candidates, we evaluated the change in proteomic intensities among groups based on cancer invasion in all the proteomic data, including that of label-free LBC and the cell line TMT (Figure 3B, Table S9). Seven out of the 12 candidates showed a random alteration of protein intensity regardless of the advanced tumor stage in BUC patients and of invasive phenotype in cell lines, which were eventually excluded for further validation tests. The remaining five candidate biomarkers, namely, *GRHL2*, *LLGL2*, *MSN*, *NCAM2*, and *VAPA*, demonstrated a gradual increase of protein intensity in groups with more invasive phenotypes, which guided us to select them as the final candidates for further validation.

In gene ontology analysis, the five final candidate biomarkers were associated with cellular transport (*LLGL2* and *VAPA*), immune response (*VAPA*), invasion process (*LLGL2* and *MSN*), and cellular organization (*GRHL2* and *MSN*) (Figure 3C). All four candidates, except *MSN*, were downregulated in MIBUC. *GRHL2* affects cell morphogenesis and epithelial–mesenchymal transition (EMT) and acts as a tumor suppressor in various tumors [22,45]. *LLGL2* and *VAPA* are involved in cellular transport and affect invasion process. These genes show a tumor-suppressive role in various tumors [21,24]. On the other hand, *MSN* expression was upregulated in MIBUC and consistent with its oncogenic role in invasion process [16,18,19].

2.4. The Inhibitory Effect of Moesin (*MSN*) Depletion on Cancer Invasion in BUC

Next, we performed a two-dimensional (2D) invasion and migration assay with T24 and J82 BUC cell lines to evaluate how the five selected candidates modulated the invasion ability of BUC cells (Figure 4A). The invasion and migration assay showed that BUC cells were significantly reduced in both the *MSN*-depleted cell lines as opposed to other candidate biomarkers including *LLGL2*, *NCAM2*, and *VAPA* that all failed to prove significant alteration of invasion ability (Figure S3). A further 3D invasion assay showed concordant findings that *MSN* knockdown T24 and J82 BUC cells exhibited a remarkable reduction in cell invasion (Figure 4B,C). A further pre-ranked gene enrichment analysis utilizing gene ontology term-defined gene sets linked *MSN* to proteins involved in actin dynamics (*CORO1A*, *FLNA*, and *LCPI*), formin (*FMNL1*), integrin signaling (*FERMT3*, *ITGAM*, *ITGA6*, and *ITGB4*), extracellular matrix (ECM) remodeling (*MMP9*), EMT phenotype (*VIM*), small GTPase activator (*ARHGEF2*), and mitogen-activated protein kinase (MAPK) pathway (*MAP2K1*) that were upregulated in the MIBUC group (Figure 5). A further co-expression analysis using TCGA data revealed strong correlation of *MSN* expression with proteins involved in actin dynamics (*FLNA*), integrin signaling (*ITGAM*), and EMT phenotype (*VIM*) and suggested a co-operative role of *MSN* with signaling pathways associated with cell motility (Figure S4).

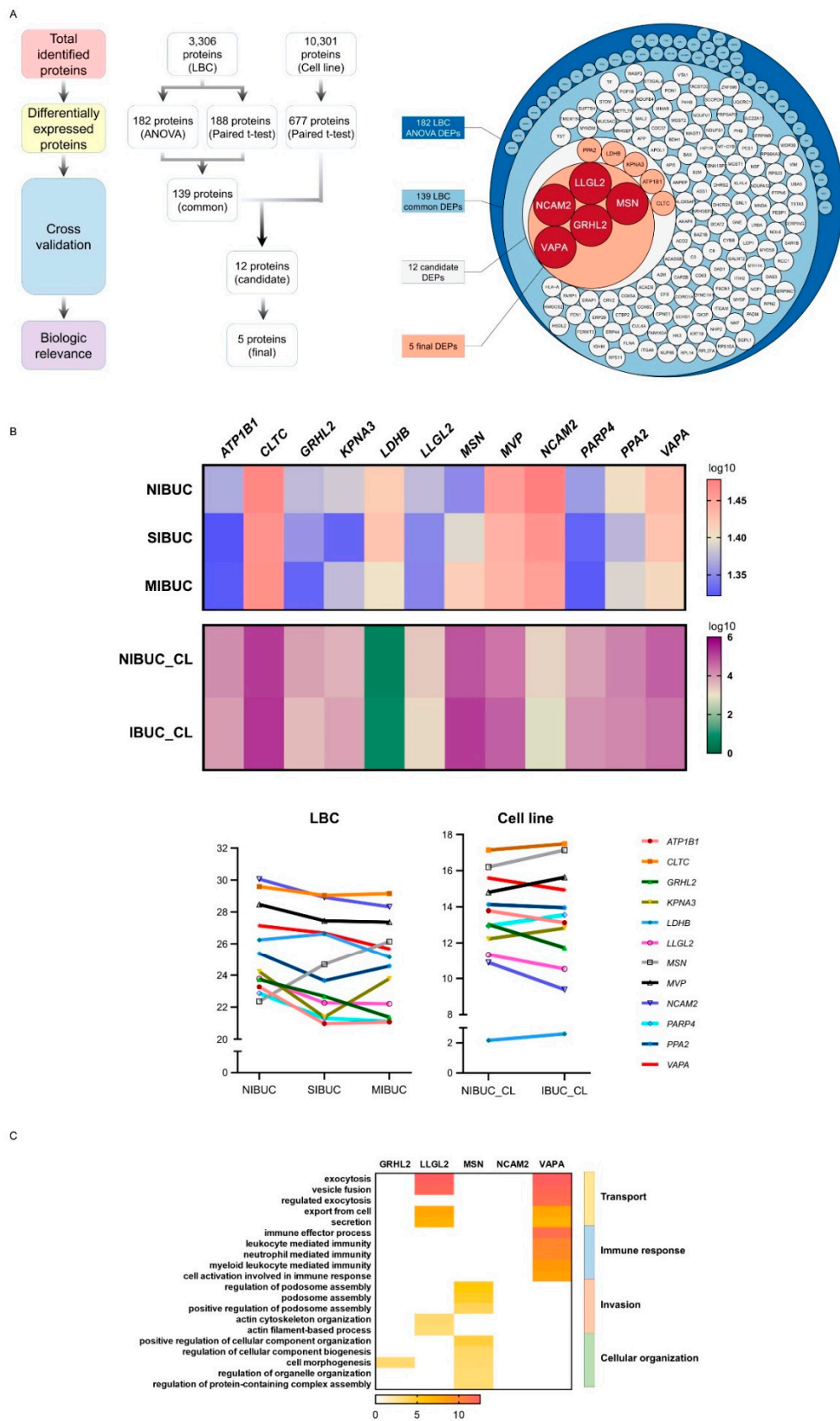


Figure 3. Invasion-associated biomarker selection. (A) Workflow for biomarker selection (left, overview; right, circlepack). (B) Intensity tendency of candidate biomarkers in BUC LBC and cell line proteomics (left, heatmap; right, broken-line graph). (C) Gene ontology results of final five candidate biomarkers.

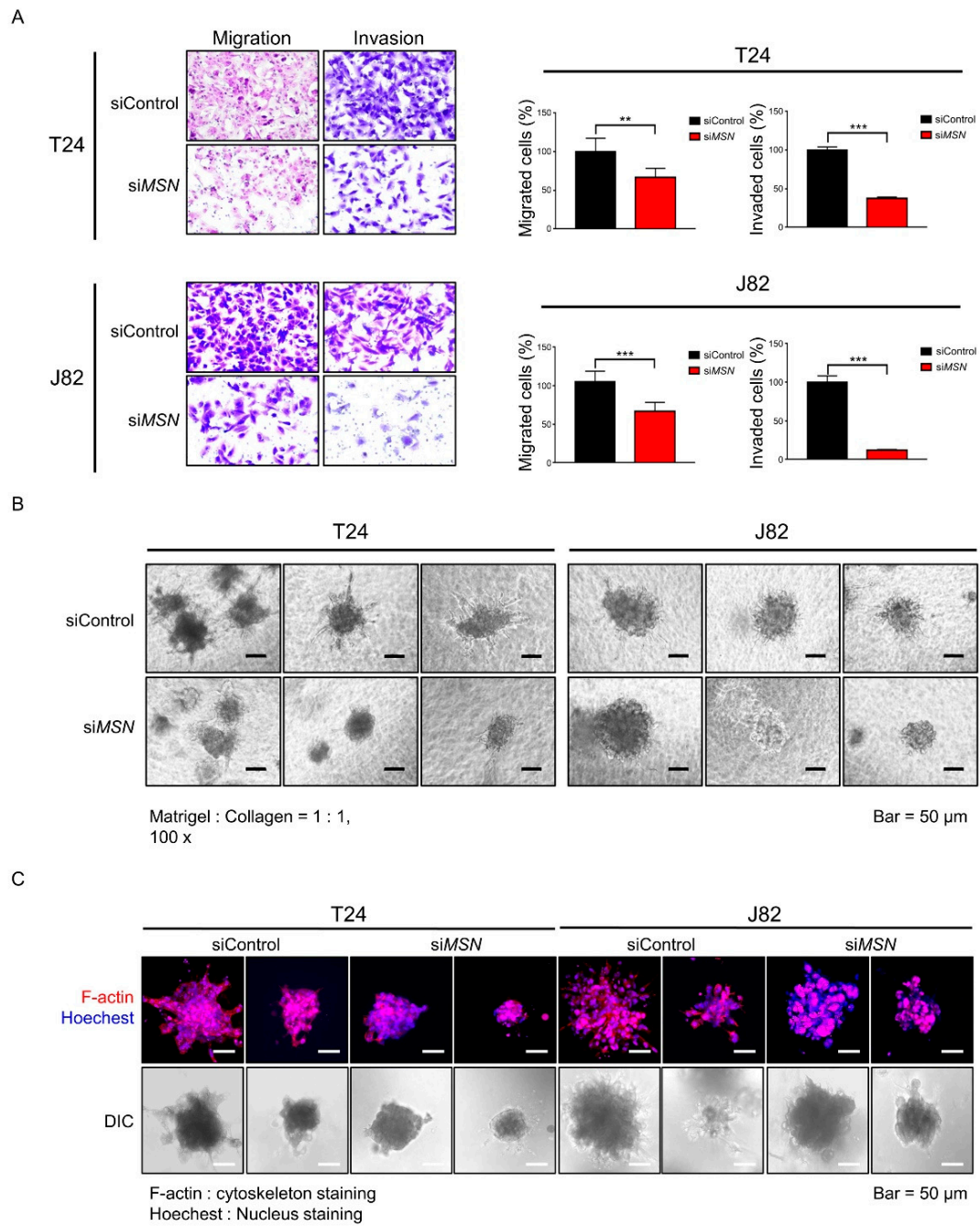


Figure 4. Functional validation of invasive role of MSN with small interfering RNAs (siRNAs) using two-dimensional (2D) and three-dimensional (3D) migration and invasion assays. **(A)** 2D migration and invasion assay (statistical significance, ** p -value < 0.01; *** p -value < 0.001). **(B)** Phase-contrast microscope image of 3D dissemination. **(C)** Confocal microscope image of 3D dissemination.

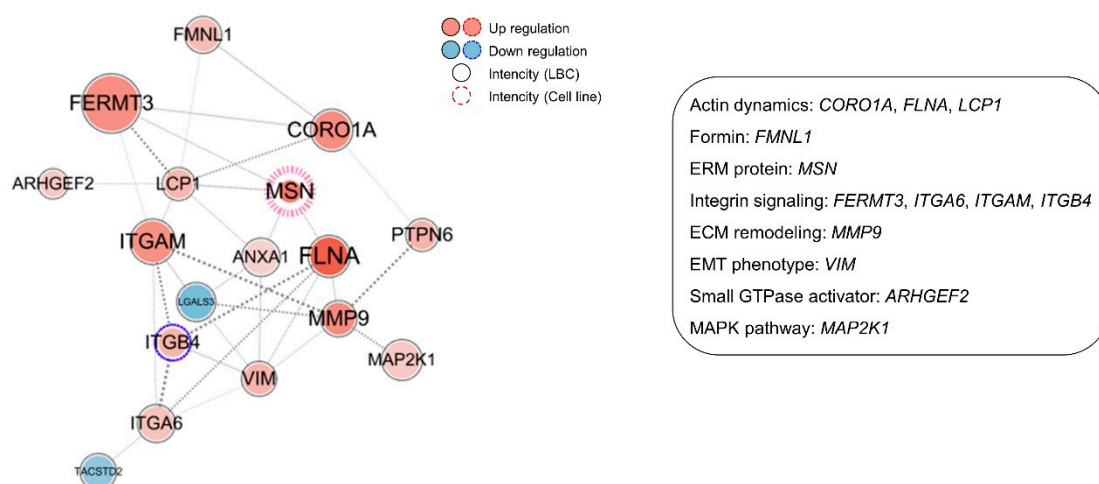


Figure 5. Protein-protein interaction based-network analysis with differentially expressed proteins (DEPs) between muscle-invasive bladder urothelial carcinoma (MIBUC) and non-invasive bladder urothelial carcinoma (NIBUC) in cell motility.

2.5. Slide-Based Moesin Immunocytochemical Test Predicts Invasive Urothelial Carcinoma on Urine Liquid-Based Cytology

We further verified the diagnostic role of moesin to predict BUC invasion and its clinical application through ICC based on an independent urine LBC cohort, which was composed of NIBUC, SIBUC, and MIBUC. The proportion of moesin immunoreactivity significantly increased with BUC invasion—38.5%, 80.0%, and 85.7% in NIBUC, SIBUC, and MIBUC, respectively (p -value = 0.046; Figure 6, Table 1). The predictive ability was more powerful in a dichotomous comparison between the BUC group without invasion and the other group with invasion (p -value = 0.023, moesin immunoreactive rates, 38.5% vs. 82.4%, respectively).

Table 1. Correlation between moesin immunocytochemistry (ICC) and invasion depth of bladder urothelial carcinoma (BUC).

	Moesin Immunoreactivity, n (%)		p -Value	H-Score	p -Value
	Negative ($n = 11$)	Positive ($n = 19$)			
NIBUC ($n = 13$)	8 (72.7)	5 (26.3)	0.046	56.15	0.042
SIBUC ($n = 10$)	2 (18.2)	8 (42.1)		133.50	
MIBUC ($n = 7$)	1 (9.1)	6 (31.6)		165.71	
NIBUC ($n = 13$)	8 (72.7)	5 (26.3)	0.023	56.15	0.014
IBUC ($n = 17$)	3 (27.3)	14 (73.7)		146.76	

Abbreviations: IBUC, invasive bladder urothelial carcinoma; MIBUC, muscle-invasive bladder urothelial carcinoma; NIBUC, non-invasive bladder urothelial carcinoma; SIBUC, stromal invasive bladder urothelial carcinoma.

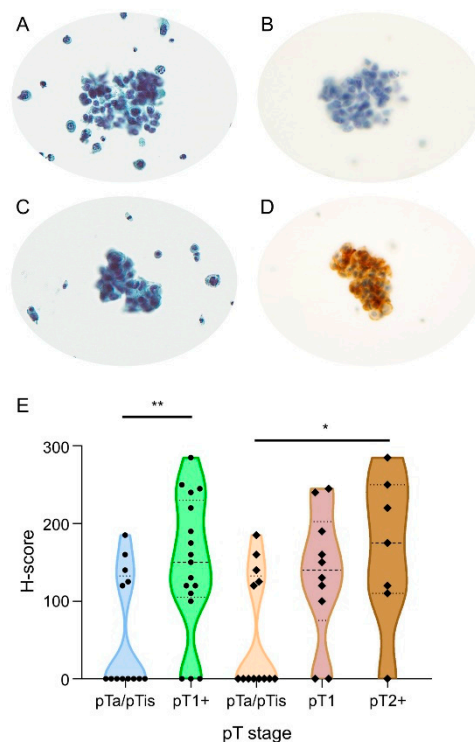


Figure 6. Immunocytochemical (ICC) verification of moesin (*MSN*) as a predictive biomarker for invasive bladder urothelial carcinoma (BUC) in liquid-based cytology (LBC) samples. (A–D) Representative BUC and moesin ICC images on LBC: (A) BUC LBC image, (B) matched ICC image (negative staining), (C) BUC LBC image, (D) matched ICC image (positive staining). (E) Moesin ICC positivity among non-invasive BUC (NIBUC) (pTa/pTis), stromal-invasive BUC (SIBUC) (pT1), and muscle-invasive BUC (MIBUC) (pT2+) (statistical significance, * p -value < 0.05; ** p -value < 0.01; pT, pathologic T; pTa, non-invasive papillary carcinoma; pTis, urothelial carcinoma in situ; pT1, tumor invades lamina propria (subepithelial connective tissue); pT2+, tumor invades muscularis propria and beyond).

3. Discussion

In this study, we prioritized moesin (*MSN*) as a protein biomarker for early detection of BUC invasion using a liquid-based cytologic test, which is the most widely used clinical screening method for monitoring bladder cancer progression. Moesin showed predictive ability for invasion of BUC in the independent ICC cohort. In situ immunoreactivities of moesin on LBC slide-based tests revealed statistical discriminative power when more than one cell was immunostained in LBC slides, which was concordant with the previous study where positive immunostaining in any cancer cell was significantly associated with poor overall survival in BUC [17]. In the TCGA public dataset, the higher expression of *MSN* transcript was also marginally associated with unfavorable clinical outcomes (p -value = 0.061; Figure S5). The higher expression of *MSN* was also associated with advanced American Joint Committee on Cancer (AJCC) staging (p -value = 0.001) and angiolymphatic invasion (p -value = 0.050) (Table S10).

Growing evidence has shown that moesin (*MSN*) plays a crucial role in invasion by cytoskeletal reorganization and EMT in various malignant tumors [16,18,19]. Although the functional relevance of *MSN* has not been fully revealed in urothelial carcinoma [9,17], our in vitro 3D spheroid invasion assay along with the 2D invasion assay confirmed significantly decreased invasion ability in *MSN*-depleted BUC cell lines. The 3D tumor spheroid invasion assay has advantages, for example, tumor spheroids mimic a more physiologic tissue-like morphology and recapitulate tumor cells and microenvironment [46,47]

Our proteomic data demonstrated that moesin (*MSN*) upregulation is one of the major factors for BUC invasion, which can be more critical as the previous proteomic analysis of urine extracellular vesicles revealed moesin as one of the candidate biomarkers for bladder cancer diagnosis [9]. In a further network analysis with protein–protein interactions, we confirmed a tight clustering of *MSN* with several key proteins, including *ITGA6*, *ITGB4*, *FERMT3*, *FLNA*, *LCPI*, *CORO1A*, *FMNL1*, *ARHGEF2*, and *MMP9*, all of which modulate membrane ruffling, lamellipodia and filopodia formation, cell–ECM interaction, and ECM remodeling that play a crucial role in cancer cell invasion [48] (Figure S6). Moesin binds to phosphatidylinositol 4,5-bisphosphate (PI(4,5)P₂), CD44, and Na⁺/H⁺ exchanger 1 (NHE-1), which are all key factors for cytoskeletal reorganization by modulating integrin signaling and integrin complex formation [16]. The complex that consists of integrin subunit α6 (*ITGA6*) and subunit β4 (*ITGB4*) and sequentially interacts with laminin [49] and kindlin-3 (*FERMT3*) is involved in tumorigenesis by modulating tumor cell–ECM interaction [50]. Filamin A (*FLNA*), plastin-2 (*LCPI*), coronin-1A (*CORO1A*), and formin-like-1 (*FMNL1*) also affect cytoskeletal dynamics by modulating actin filaments which eventually prompt cancer mobility and invasion [51,52]. Additional molecular studies need to be carried out, focusing on the above-selected proteomic markers. The results and how they can be interpreted in perspective of previous studies and working hypotheses should be discussed. The findings and their implications should be discussed in the broadest context possible. Future research directions may also be highlighted.

4. Materials and Methods

4.1. Patient Selection and Clinicopathologic Review

A total of 16 surgically confirmed LBC samples and an independent BUC cohort of 30 LBC specimens encompassing NIBUC, SIBUC, and MIBUC were employed for quantitative proteomic analysis and verification of diagnostic utility of ICC, respectively (Table 2). This study was approved by the Institutional Review Board of Seoul National University Hospital (IRB No. H-1602-150-747). Detailed information can be found in the Supplementary Methods.

Table 2. Clinicopathologic features of bladder urothelial carcinoma (BUC) in liquid-based cytology (LBC) samples.

	Proteomic Analysis			ICC Validation		
	NIBUC, n (%)	SIBUC, n (%)	MIBUC, n (%)	NIBUC, n (%)	SIBUC, n (%)	MIBUC, n (%)
	n = 6	n = 5	n = 5	n = 13	n = 10	n = 7
Age (years)						
50-60	0 (0.0)	1 (20)	0 (0)	2 (15.4)	1 (10)	1 (14.3)
60-70	5 (83.3)	2 (40)	4 (80)	7 (53.8)	2 (20)	2 (28.6)
>70	1 (16.7)	2 (40)	1 (20)	4 (30.8)	7 (70)	4 (57.1)
Gender						
Male	5 (83.3)	5 (100)	5 (100)	12 (92.3)	10 (100)	6 (85.7)
Female	1 (16.7)	0 (0)	0 (0)	1 (7.7)	0 (0)	1 (14.3)
Pathologic diagnosis						
Suspicious for high-grade urothelial carcinoma	5 (83.3)	3 (60)	4 (80)	8 (61.5)	2 (20)	2 (28.6)
High-grade urothelial carcinoma	1 (16.7)	2 (40)	1 (20)	5 (38.5)	8 (80)	5 (71.4)
Papillary urothelial carcinoma, high-grade	6 (100)	4 (80)	0 (0)	13 (100)	10 (100)	3 (42.9)
Invasive urothelial carcinoma, high grade	0 (0)	1 (20)	5 (100)	0 (0)	0 (0)	4 (57.1)
Concurrent carcinoma in situ	1 (16.7)	2 (40)	1 (20)	5 (38.5)	3 (30)	0 (0)

Table 2. Cont.

	Proteomic Analysis			ICC Validation		
	NIBUC, <i>n</i> (%)	SIBUC, <i>n</i> (%)	MIBUC, <i>n</i> (%)	NIBUC, <i>n</i> (%)	SIBUC, <i>n</i> (%)	MIBUC, <i>n</i> (%)
	<i>n</i> = 6	<i>n</i> = 5	<i>n</i> = 5	<i>n</i> = 13	<i>n</i> = 10	<i>n</i> = 7
pT stage						
pTa/pTis	6 (100)	0 (0)	0 (0)	13 (100)	0 (0)	0 (0)
pT1	0 (0)	5 (100)	0 (0)	0 (0)	10 (100)	0 (0)
pT2+	0 (0)	0 (0)	5 (100)	0 (0)	0 (0)	7 (100)
AJCC stage						
0a/0is	6 (100)	0 (0)	0 (0)	13 (100)	0 (0)	0 (0)
I	0 (0)	5 (100)	0 (0)	0 (0)	10 (100)	0 (0)
II+	0 (0)	0 (0)	5 (100)	0 (0)	0 (0)	7 (100)
Treatment						
Transurethral resection	6 (100)	5 (100)	1 (20)	13 (100)	10 (100)	1 (14.3)
Radical cystectomy	0 (0)	0 (0)	4 (80)	0 (0)	0 (0)	6 (85.7)

Abbreviations: AJCC, American Joint Committee on Cancer; ICC, immunocytochemistry; MIBUC, muscle-invasive bladder urothelial carcinoma; NIBUC, non-invasive bladder urothelial carcinoma; pT, pathologic T; pTa, non-invasive papillary carcinoma; pTis, urothelial carcinoma in situ; pT1, tumor invades lamina propria (subepithelial connective tissue); pT2+, tumor invades muscularis propria and beyond; SIBUC, stromal invasive bladder urothelial carcinoma.

4.2. Proteomics Analysis and Data Processing for Peptide Identification

Figure S7 indicates the key steps in our approach for the proteomic discovery of novel biomarkers. Tumor cells from LBC slides were scraped and the peptide was digested using the filter-aided sample preparation (FASP) procedure as previously described [53]. Each sample was desalted [54] and was followed by LC-MS/MS analysis. For BUC cell lines, a proteomic analysis was performed after eight BUC cell lines, namely, T24, J82, 253J-BV, 253J, 5637, RT4, HT1376, and HT1197 (ATCC; Manassas, VA, USA), were categorized as IBUC_CL and NIBUC_CL based on their invasion and migration capacities. Each sample was labeled by TMT and was followed by LC-MS/MS analysis. The LC-MS/MS analysis was conducted using a Q Exactive Plus Hybrid Quadrupole-Orbitrap mass spectrometer (Thermo Fisher Scientific Inc., Waltham, MA, USA) and an Ultimate 3000 RSLC system (Dionex, Sunnyvale, CA, USA) as previously described [53,55]. MaxQuant version 1.5.3.1 (Max Planck Institute of Biochemistry, Munich, Germany) [56] with the Andromeda search engine [57] and Proteome Discoverer 2.1 software (Thermo Fisher Scientific Inc., Waltham, MA, USA) [58] with the SEQUEST-HT search engine were employed for processing LBC and cell line data, respectively. More detailed information is available in the Supplementary Methods.

4.3. Cell Migration and Invasion Assays with Small Interfering RNA (siRNA) Transfection

The T24 and J82 BUC cell lines were selected to evaluate cell migration and invasion abilities. RNA interference siRNAs targeting *GRHL2*, *LLGL2*, *MSN*, *NCAM2*, and *VAPA* were employed, followed by transfection to BUC cells. Detailed information is available in the Supplementary Methods.

4.4. Tumor Spheroids and 3D Spheroid Invasion Assay

Tumor spheroids were generated for suspension culture. Mixed collagen/Matrigel matrices were constructed as previously described [59]. The dissemination of spheroids was assessed under a phase-contrast microscope. A confocal laser scanning microscope (Leica TCS SP8; Leica microsystems, Wetzlar, Germany) was employed for the detection of stained F-actin. Phalloidin–rhodamine (Thermo Fisher Scientific Inc., Waltham, MA, USA; 1:100 in phosphate-buffered saline (PBS)) was used for visualization of the actin cytoskeleton in 3D spheroid cells. Supplementary Methods contain additional information.

4.5. Immunocytochemical Analysis

Immunocytochemical staining was conducted on LBC slides. Immunostaining of moesin was performed using Benchmark XT (Ventana Medical System, Inc., Tucson, AZ, USA). A monoclonal mouse anti-moesin antibody (Santa Cruz Biotechnology, Dallas, TX, USA) was diluted to 1:500. The binding of the primary antibody was identified using an Optiview universal DAB kit (Ventana Medical Systems, Inc., Tucson, AZ, USA) according to the manufacturer's protocol. ICC analysis defined negative expression for tumor cells with no moesin expression as opposed to positive expression when at least more than one tumor cell expressed moesin [17]. We also assessed the intensity and proportion of positive BUC cells for H-score evaluation [60].

4.6. Statistical Analyses

All proteomic datasets were submitted to the ProteomeXchange Consortium (<http://proteomecentral.proteomechange.org>) (project ID: PXD016437) [61]. TopGene Suite resources (<https://toppgene.cchmc.org/>) [62] and String [63] were used for gene ontology annotation and interaction network model construction, respectively. Cytoscape version 3.7.1 (Institute for Systems Biology, Seattle, WA, USA) [64] was used for the illustration of the network model. Statistical analyses were conducted using the Perseus software (Max Planck Institute of Biochemistry, Munich, Germany) [65] for proteomic data. The H-score for ICC validation was analyzed by utilizing the Kruskal–Wallis test and Mann–Whitney *U* test for the comparison of BUC groups with the GraphPad Prism 8.0 program (GraphPad Software, Inc., CA, USA). The cross-tabulation analysis was conducted by Pearson's χ^2 test and Fisher exact test with IBM SPSS Statistics version 20 (IBM Corp., Armonk, NY, USA). Detailed information is available in Supplementary Methods.

5. Conclusions

Taking advantage of advanced proteomic techniques, the present study identified a novel promising diagnostic biomarker that can be applied as a new ancillary test for the prediction of BUC with invasion using voided urine LBC samples, the most frequently used diagnostic sample in routine practice. We successfully demonstrated that the immunoreactivity of moesin can be utilized as a diagnostic marker for early surgical intervention. Further investigation will be necessary for our future studies to validate the predictive ability of moesin in a larger cohort.

Supplementary Materials: The following are available online at <http://www.mdpi.com/2072-6694/12/4/1018/s1>, Figure S1: Identified and quantified proteins among 16 bladder urothelial carcinoma (BUC) liquid-based cytology (LBC) samples (duplicated analyses for each sample; 1-12, non-invasive BUC (NIBUC); 13-22, stromal-invasive BUC (SIBUC); 23-32, muscle-invasive BUC (MIBUC)), Figure S2: Hierarchical clustering and gene ontology results between two groups from bladder urothelial carcinoma (BUC) liquid-based cytology (LBC) samples (A) Hierarchical clustering and volcano plot between two groups from BUC LBC samples (left, stromal-invasive BUC (SIBUC) and non-invasive BUC (NIBUC); right, muscle-invasive BUC (MIBUC) and SIBUC). (B) gene ontology results between two groups from BUC LBC samples (left, SIBUC and NIBUC; right, MIBUC and SIBUC), Figure S3: Functional validation of invasive role of *LLGL2*, *NCAM2*, and *VAPA* with small interfering RNA (siRNA) using two-dimensional (2D) and three-dimensional (3D) invasion assays. (A) 2D invasion assay (statistical significance, *** *p*-value < 0.001), (B) confocal microscope image of 3D dissemination, Figure S4: Co-expression analysis of *MSN* with key proteins in signaling pathway associated with cell motility. (A) Actin dynamics, (B) formin, (C) integrin signaling, (D) extracellular matrix (ECM) remodeling, (E) epithelial–mesenchymal transition (EMT) phenotype, (F) small GTPase activator, (G) MAPK pathway, (H) others, Figure S5: Kaplan–Meier survival curve for overall survival according to *MSN* RNA expression on The Cancer Genome Atlas (TCGA) public data, Figure S6: Proposed cellular aspect of bladder urothelial carcinoma (BUC) invasion process. (A) Overview of BUC invasion process, (B) lamellipodia formation, (C) filopodia formation, (D) rear retraction (abbreviations: C-ERMAD, C-terminal ERM-associated domain; ECM, extracellular matrix; FAK, focal adhesion kinase; FERM, 4.1-band ERM; FGFR3, fibroblast growth factor receptor 3; GDP, guanosine diphosphate; GTP, guanosine triphosphate; ILK, integrin-linked kinase; integrin (BC, bent-closed; EC, extended-closed; EO, extended-open); MAPK, mitogen-activated protein kinase; MMPs, matrix metalloproteinases; PI(4,5)P₂, phosphatidylinositol 4,5-bisphosphate; ROCK, Rho-associated protein kinase; RTK, receptor tyrosine kinase; TGF- β , transforming growth factor β ; VT, vimentin), Figure S7: Overall workflow of the study design. Proteomic analysis of bladder urothelial carcinoma (BUC) liquid-based cytology (LBC) samples and cell line samples with invasion assay and immunocytochemistry (ICC) validation, Table S1: Total list of identified protein groups in bladder urothelial carcinoma (BUC) (liquid-based cytology

(LBC) samples), Table S2: Total list of differentially expressed proteins (DEPs) by ANOVA in bladder urothelial carcinoma (BUC) (liquid-based cytology (LBC) samples), Table S3: Total list of differentially expressed proteins (DEPs) by pairwise t-test in bladder urothelial carcinoma (BUC) (liquid-based cytology (LBC) samples), Table S4: Gene ontology (GO) analysis of differentially expressed proteins (DEPs) in bladder urothelial carcinoma (BUC) (liquid-based cytology (LBC) samples), Table S5: Gene ontology (GO) analysis of differentially expressed proteins (DEPs) with upregulation in bladder urothelial carcinoma (BUC), Table S6: Gene ontology (GO) analysis of differentially expressed proteins (DEPs) with downregulation in bladder urothelial carcinoma (BUC) (liquid-based cytology (LBC) samples), Table S7: Total list of identified protein groups in tandem mass tag (TMT)-based proteomics of bladder urothelial carcinoma (BUC) cell lines, Table S8: Total list of differentially expressed proteins (DEPs) in tandem mass tag (TMT)-based proteomics of bladder urothelial carcinoma (BUC) cell lines, Table S9: Comparison of differentially expressed proteins (DEPs) between proteomics of liquid-based cytology (LBC) samples of bladder urothelial carcinoma (BUC) and tandem mass tag (TMT)-based proteomics of BUC cell lines, Table S10: Correlation between *MSN* RNA expression and AJCC staging and angiolymphatic invasion in bladder urothelial carcinoma (BUC) in The Cancer Genome Atlas (TCGA) public data.

Author Contributions: Conceptualization, J.H.P., C.L., D.H., J.S.L., and H.S.R.; data curation, J.H.P., D.H., K.M.L., M.J.S., K.K., H.L. (Heonyi Lee), M.J., J.H.M., and H.S.R.; formal analysis, J.H.P., D.H., K.M.L., H.L. (Heonyi Lee), K.C.M., Y.K., and H.S.R.; funding acquisition, C.L., J.S.L., and H.L. (Hyebin Lee); investigation, J.H.P., D.H., K.M.L., H.L. (Heonyi Lee), Y.K., and H.S.R.; methodology, J.H.P., D.H., K.M.L., K.K., Y.K., and H.S.R.; project administration, H.S.R.; resources, H.L. (Heonyi Lee), K.C.M., M.J., and J.H.M.; supervision, J.S.L., H.L. (Hyebin Lee), and H.S.R.; validation, J.H.P., K.M.L., and H.S.R.; visualization, J.H.P., M.J.S., and H.L. (Heonyi Lee); writing—original draft, J.H.P.; writing—review and editing, J.H.P., C.L., J.S.L., and H.S.R. All authors have read and agreed to the published version of the manuscript.

Funding: This research was funded by grant 2620170040 from the Seoul National University Hospital Research Fund, the National Research Foundation of Korea (NRF) funded by the Ministry of Science, ICT and Future Planning (NRF-2017R1C1B5017694 and 2019R1C1C1006640).

Conflicts of Interest: The authors declare no conflicts of interest.

Abbreviations

2D	2-dimensional
3D	3-dimensional
AJCC	American Joint Committee on Cancer
BCG	bacillus Calmette–Guérin
BUC	bladder urothelial carcinoma
C-ERMAD	C-terminal ERM-associated domain
DEPs	differentially expressed proteins
ECM	extracellular matrix
EMT	epithelial–mesenchymal transition
ERM	ezrin, radixin, and moesin
FASP	filter-aided sample preparation
FDR	false discovery rate
FERM	4.1-band ERM
GO	gene ontology
HCD	higher-energy collisional dissociation
HGUC	high-grade urothelial carcinoma
IBUC_CL	invasive bladder urothelial carcinoma cell line
ICC	immunocytochemistry
LBC	liquid-based cytology
LC-MS/MS	liquid chromatography-tandem mass spectrometry
LFQ	label-free quantification
MAPK	mitogen-activated protein kinase
MIBUC	muscle-invasive bladder urothelial carcinoma
NHE-1	Na ⁺ /H ⁺ exchanger 1
NIBUC	non-invasive bladder urothelial carcinoma
NIBUC_CL	non-invasive bladder urothelial carcinoma cell line
PBS	phosphate-buffered saline
PI(4,5)P ₂	phosphatidylinositol 4,5-bisphosphate

poly-HEMA	poly(2-hydroxyethyl methacrylate)
pT	pathologic T
pTa	non-invasive papillary carcinoma
pTis	urothelial carcinoma in situ
pT1	tumor invades lamina propria (subepithelial connective tissue)
pT2+	tumor invades muscularis propria and beyond
SDS	sodium dodecyl sulfate
SHGUC	suspicious for high-grade urothelial carcinoma
SIBUC	stromal-invasive bladder urothelial carcinoma
siRNA	small interfering RNA
TCGA	The Cancer Genome Atlas
TCEP	tris(2-carboxyethyl)phosphine
TFA	trifluoroacetic acid
TMT	tandem mass tag
TUR-B	transurethral resection of bladder

References

1. Grignon, D.J.; Al-Ahmadie, H.; Algaba, F.; Amin, M.B.; Comp erat, E.; Dyrskj t, L.; Epstein, J.I.; Hansel, D.E.; Kn uchel, R.; Lloreta, J.; et al. Urothelial tumours: Infiltrating urothelial carcinoma. In *WHO Classification of Tumours of the Urinary System and Male Genital Organs*, 4th ed.; Moch, H., Humphrey, P.A., Ulbright, T.M., Reuter, V.E., Eds.; International Agency for Research on Cancer: Lyon, France, 2016; pp. 81–98.
2. Clark, P.E.; Agarwal, N.; Biagioli, M.C.; Eisenberger, M.A.; Greenberg, R.E.; Herr, H.W.; Inman, B.A.; Kuban, D.A.; Kuzel, T.M.; Lele, S.M.; et al. Bladder cancer. *J. Natl. Compr. Cancer Netw.* **2013**, *11*, 446–475. [[CrossRef](#)]
3. Zhang, S.; Liu, Y.; Liu, Z.; Zhang, C.; Cao, H.; Ye, Y.; Wang, S.; Zhang, Y.; Xiao, S.; Yang, P.; et al. Transcriptome profiling of a multiple recurrent muscle-invasive urothelial carcinoma of the bladder by deep sequencing. *PLoS ONE* **2014**, *9*, e91466. [[CrossRef](#)] [[PubMed](#)]
4. Cancer Genome Atlas Research Network. Comprehensive molecular characterization of urothelial bladder carcinoma. *Nature* **2014**, *507*, 315–322. [[CrossRef](#)] [[PubMed](#)]
5. Grau, L.; Luque-Garcia, J.L.; Gonz alez-Peramato, P.; Theodorescu, D.; Palou, J.; Fernandez-Gomez, J.M.; S anchez-Carbayo, M. A quantitative proteomic analysis uncovers the relevance of CUL3 in bladder cancer aggressiveness. *PLoS ONE* **2013**, *8*, e53328. [[CrossRef](#)] [[PubMed](#)]
6. De Velasco, G.; Trilla-Fuertes, L.; Gamez-Pozo, A.; Urbanowicz, M.; Ruiz-Ares, G.; Sep ulveda, J.M.; Prado-Vazquez, G.; Arevalillo, J.M.; Zapater-Moros, A.; Navarro, H.; et al. Urothelial cancer proteomics provides both prognostic and functional information. *Sci. Rep.* **2017**, *7*, 15819. [[CrossRef](#)] [[PubMed](#)]
7. Latosinska, A.; Mokou, M.; Makridakis, M.; Mullen, W.; Zoidakis, J.; Lygirou, V.; Frantzi, M.; Katafigiotis, I.; Stravodimos, K.; Hupe, M.C.; et al. Proteomics analysis of bladder cancer invasion: Targeting EIF3D for therapeutic intervention. *Oncotarget* **2017**, *8*, 69435–69455. [[CrossRef](#)]
8. Latosinska, A.; Makridakis, M.; Frantzi, M.; Borr as, D.M.; Janssen, B.; Mullen, W.; Zoidakis, J.; Merseburger, A.S.; Jankowski, V.; Mischak, H.; et al. Integrative analysis of extracellular and intracellular bladder cancer cell line proteome with transcriptome: Improving coverage and validity of -omics findings. *Sci. Rep.* **2016**, *6*, 25619. [[CrossRef](#)]
9. Lee, J.; McKinney, K.Q.; Pavlopoulos, A.J.; Niu, M.; Kang, J.W.; Oh, J.W.; Kim, K.P.; Hwang, S. Altered Proteome of Extracellular Vesicles Derived from Bladder Cancer Patients Urine. *Mol. Cells* **2018**, *41*, 179–187.
10. Strogilos, R.; Mokou, M.; Latosinska, A.; Makridakis, M.; Lygirou, V.; Mavrogeorgis, E.; Drekolias, D.; Frantzi, M.; Mullen, W.; Fragkoulis, C.; et al. Proteome-based classification of Nonmuscle Invasive Bladder Cancer. *Int. J. Cancer* **2020**, *146*, 281–294. [[CrossRef](#)]
11. Lee, H.; Kim, K.; Woo, J.; Park, J.; Kim, H.; Lee, K.E.; Kim, H.; Kim, Y.; Moon, K.C.; Kim, J.Y.; et al. Quantitative Proteomic Analysis Identifies AHNAK (Neuroblast Differentiation-associated Protein AHNAK) as a Novel Candidate Biomarker for Bladder Urothelial Carcinoma Diagnosis by Liquid-based Cytology. *Mol. Cell. Proteom.* **2018**, *17*, 1788–1802. [[CrossRef](#)]

12. Brown, F.M. Urine cytology. It is still the gold standard for screening? *Urol. Clin. N. Am.* **2000**, *27*, 25–37. [[CrossRef](#)]
13. Clark, P.E.; Spiess, P.E.; Agarwal, N.; Bangs, R.; Boorjian, S.A.; Buyyounouski, M.K.; Efstathiou, J.A.; Flaig, T.W.; Friedlander, T.; Greenberg, R.E.; et al. NCCN Guidelines Insights: Bladder Cancer, Version 2.2016. *J. Natl. Compr. Cancer Netw.* **2016**, *14*, 1213–1224. [[CrossRef](#)] [[PubMed](#)]
14. Allison, D.B.; VandenBussche, C.J. A Review of Urine Ancillary Tests in the Era of the Paris System. *Acta Cytol.* **2020**, *64*, 182–192. [[CrossRef](#)] [[PubMed](#)]
15. Tsukita, S.; Yonemura, S.; Tsukita, S. ERM proteins: Head-to-tail regulation of actin-plasma membrane interaction. *Trends Biochem. Sci.* **1997**, *22*, 53–58. [[CrossRef](#)]
16. Clucas, J.; Valderrama, F. ERM proteins in cancer progression. *J. Cell Sci.* **2014**, *127*, 267–275. [[CrossRef](#)]
17. Sanchez-Carbayo, M.; Socci, N.D.; Charytonowicz, E.; Lu, M.; Prystowsky, M.; Childs, G.; Cordon-Cardo, C. Molecular profiling of bladder cancer using cDNA microarrays: Defining histogenesis and biological phenotypes. *Cancer Res.* **2002**, *62*, 6973–6980.
18. Carmeci, C.; Thompson, D.A.; Kuang, W.W.; Lightdale, N.; Furthmayr, H.; Weigel, R.J. Moesin expression is associated with the estrogen receptor-negative breast cancer phenotype. *Surgery* **1998**, *124*, 211–217. [[CrossRef](#)]
19. Wang, Q.; Lu, X.; Zhao, S.; Pang, M.; Wu, X.; Wu, H.; Hoffman, R.M.; Yang, Z.; Zhang, Y. Moesin Expression Is Associated with Glioblastoma Cell Proliferation and Invasion. *Anticancer Res.* **2017**, *37*, 2211–2218. [[CrossRef](#)]
20. Uhlen, M.; Zhang, C.; Lee, S.; Sjöstedt, E.; Fagerberg, L.; Bidkhor, G.; Benfeitas, R.; Arif, M.; Liu, Z.; Edfors, F.; et al. A pathology atlas of the human cancer transcriptome. *Science* **2017**, *357*, eaan2507. [[CrossRef](#)]
21. Mertens, D.; Wolf, S.; Schroeter, P.; Schaffner, C.; Döhner, H.; Stilgenbauer, S.; Lichter, P. Down-regulation of candidate tumor suppressor genes within chromosome band 13q14.3 is independent of the DNA methylation pattern in B-cell chronic lymphocytic leukemia. *Blood* **2002**, *99*, 4116–4121. [[CrossRef](#)]
22. Tay, Y.; Kats, L.; Salmena, L.; Weiss, D.; Tan, S.M.; Ala, U.; Karreth, F.; Poliseno, L.; Provero, P.; Di Cunto, F.; et al. Coding-independent regulation of the tumor suppressor PTEN by competing endogenous mRNAs. *Cell* **2011**, *147*, 344–357. [[CrossRef](#)] [[PubMed](#)]
23. Jolly, M.K.; Tripathi, S.C.; Jia, D.; Mooney, S.M.; Celiktas, M.; Hanash, S.M.; Mani, S.A.; Pienta, K.J.; Ben-Jacob, E.; Levine, H. Stability of the hybrid epithelial/mesenchymal phenotype. *Oncotarget* **2016**, *7*, 27067–27084. [[CrossRef](#)]
24. Zhang, Y.; Fang, L.; Zang, Y.; Xu, Z. Identification of Core Genes and Key Pathways via Integrated Analysis of Gene Expression and DNA Methylation Profiles in Bladder Cancer. *Med. Sci. Monit.* **2018**, *24*, 3024–3033. [[CrossRef](#)] [[PubMed](#)]
25. Barbáchano, A.; Fernández-Barral, A.; Pereira, F.; Segura, M.F.; Ordóñez-Morán, P.; Carrillo-de Santa Pau, E.; González-Sancho, J.M.; Hanniford, D.; Martínez, N.; Costales-Carrera, A.; et al. SPROUTY-2 represses the epithelial phenotype of colon carcinoma cells via upregulation of ZEB1 mediated by ETS1 and miR-200/miR-150. *Oncogene* **2016**, *35*, 2991–3003.
26. Selvakumar, P.; Owens, T.A.; David, J.M.; Petrelli, N.J.; Christensen, B.C.; Lakshmiikuttyamma, A.; Rajasekaran, A.K. Epigenetic silencing of Na, K-ATPase β 1 subunit gene ATP1B1 by methylation in clear cell renal cell carcinoma. *Epigenetics* **2014**, *9*, 579–586. [[CrossRef](#)] [[PubMed](#)]
27. Royle, S.J.; Bright, N.A.; Lagnado, L. Clathrin is required for the function of the mitotic spindle. *Nature* **2005**, *434*, 1152–1157. [[CrossRef](#)] [[PubMed](#)]
28. Raval-Fernandes, S.; Kickhoefer, V.A.; Kitchen, C.; Rome, L.H. Increased susceptibility of vault poly (ADP-ribose) polymerase-deficient mice to carcinogen-induced tumorigenesis. *Cancer Res.* **2005**, *65*, 8846–8852. [[CrossRef](#)] [[PubMed](#)]
29. Bai, H.; Wang, C.; Qi, Y.; Xu, J.; Li, N.; Chen, L.; Jiang, B.; Zhu, X.; Zhang, H.; Li, X.; et al. Major vault protein suppresses lung cancer cell proliferation by inhibiting STAT3 signaling pathway. *BMC Cancer* **2019**, *19*, 454. [[CrossRef](#)]
30. Cullis, J.; Meiri, D.; Sandi, M.J.; Radulovich, N.; Kent, O.A.; Medrano, M.; Mokady, D.; Normand, J.; Larose, J.; Marcotte, R.; et al. The RhoGEF GEF-H1 is required for oncogenic RAS signaling via KSR-1. *Cancer Cell* **2014**, *25*, 181–195. [[CrossRef](#)]
31. Satelli, A.; Li, S. Vimentin in cancer and its potential as a molecular target for cancer therapy. *Cell. Mol. Life Sci.* **2011**, *68*, 3033–3046. [[CrossRef](#)]

32. Foran, E.; McWilliam, P.; Kelleher, D.; Croke, D.T.; Long, A. The leukocyte protein L-plastin induces proliferation, invasion and loss of E-cadherin expression in colon cancer cells. *Int. J. Cancer* **2006**, *118*, 2098–2104. [[CrossRef](#)]
33. Savoy, R.M.; Ghosh, P.M. The dual role of filamin A in cancer: Can't live with (too much of) it, can't live without it. *Endocr. Relat. Cancer* **2013**, *20*, R341–R356. [[CrossRef](#)] [[PubMed](#)]
34. Sossey-Alaoui, K.; Pluskota, E.; Davuluri, G.; Bialkowska, K.; Das, M.; Szpak, D.; Lindner, D.J.; Downs-Kelly, E.; Thompson, C.L.; Plow, E.F. Kindlin-3 enhances breast cancer progression and metastasis by activating Twist-mediated angiogenesis. *FASEB J.* **2014**, *28*, 2260–2271. [[CrossRef](#)] [[PubMed](#)]
35. Boguslawska, J.; Kedzierska, H.; Poplawski, P.; Rybicka, B.; Tanski, Z.; Piekielko-Witkowska, A. Expression of Genes Involved in Cellular Adhesion and Extracellular Matrix Remodeling Correlates with Poor Survival of Patients with Renal Cancer. *J. Urol.* **2016**, *195*, 1892–1902. [[CrossRef](#)] [[PubMed](#)]
36. Castro-Castro, A.; Ojeda, V.; Barreira, M.; Sauzeau, V.; Navarro-Lérída, I.; Muriel, O.; Couceiro, J.R.; Pimentel-Muñón, F.X.; Del Pozo, M.A.; Bustelo, X.R. Coronin 1A promotes a cytoskeletal-based feedback loop that facilitates Rac1 translocation and activation. *EMBO J.* **2011**, *30*, 3913–3927. [[CrossRef](#)] [[PubMed](#)]
37. Kramer, M.W.; Kuczyk, M.A.; Hennenlotter, J.; Serth, J.; Schilling, D.; Stenzl, A.; Merseburger, A.S. Decreased expression of galectin-3 predicts tumour recurrence in pTa bladder cancer. *Oncol. Rep.* **2008**, *20*, 1403–1408. [[CrossRef](#)]
38. Choi, Y.L.; Soda, M.; Ueno, T.; Hamada, T.; Haruta, H.; Yamato, A.; Fukumura, K.; Ando, M.; Kawazu, M.; Yamashita, Y.; et al. Oncogenic MAP2K1 mutations in human epithelial tumors. *Carcinogenesis* **2012**, *33*, 956–961. [[CrossRef](#)]
39. Li, X.L.; Liu, L.; Li, D.D.; He, Y.P.; Guo, L.H.; Sun, L.P.; Liu, L.N.; Xu, H.X.; Zhang, X.P. Integrin $\beta 4$ promotes cell invasion and epithelial-mesenchymal transition through the modulation of Slug expression in hepatocellular carcinoma. *Sci. Rep.* **2017**, *7*, 40464. [[CrossRef](#)]
40. Brooks, D.L.; Schwab, L.P.; Krutilina, R.; Parke, D.N.; Sethuraman, A.; Hoogewijs, D.; Schörg, A.; Gotwald, L.; Fan, M.; Wenger, R.H.; et al. ITGA6 is directly regulated by hypoxia-inducible factors and enriches for cancer stem cell activity and invasion in metastatic breast cancer models. *Mol. Cancer* **2016**, *15*, 26. [[CrossRef](#)]
41. Varone, A.; Mariggio, S.; Patheja, M.; Maione, V.; Varriale, A.; Vessichelli, M.; Spano, D.; Formiggini, F.; Lo Monte, M.; Brancati, N.; et al. A signalling cascade involving receptor-activated phospholipase A2, glycerophosphoinositol 4-phosphate, Shp1 and Src in the activation of cell motility. *Cell Commun. Signal.* **2019**, *17*, 20. [[CrossRef](#)]
42. Katoh, M.; Katoh, M. Identification and characterization of human FMNL1, FMNL2 and FMNL3 genes in silico. *Int. J. Oncol.* **2003**, *22*, 1161–1168. [[CrossRef](#)]
43. Li, C.F.; Shen, K.H.; Huang, L.C.; Huang, H.Y.; Wang, Y.H.; Wu, T.F. Annexin-I overexpression is associated with tumour progression and independently predicts inferior disease-specific and metastasis-free survival in urinary bladder urothelial carcinoma. *Pathology* **2010**, *42*, 43–49. [[CrossRef](#)] [[PubMed](#)]
44. Nutt, J.E.; Durkan, G.C.; Mellon, J.K.; Lunec, J. Matrix metalloproteinases (MMPs) in bladder cancer: The induction of MMP9 by epidermal growth factor and its detection in urine. *BJU Int.* **2003**, *91*, 99–104. [[CrossRef](#)] [[PubMed](#)]
45. Riethdorf, S.; Frey, S.; Santjer, S.; Stoupiec, M.; Otto, B.; Riethdorf, L.; Koop, C.; Wilczak, W.; Simon, R.; Sauter, G.; et al. Diverse expression patterns of the EMT suppressor grainyhead-like 2 (GRHL2) in normal and tumour tissues. *Int. J. Cancer* **2016**, *138*, 949–963. [[CrossRef](#)] [[PubMed](#)]
46. Justus, C.R.; Leffler, N.; Ruiz-Echevarria, M.; Yang, L.V. In vitro cell migration and invasion assays. *J. Vis. Exp.* **2014**, *88*, 51046.
47. Costa, E.C.; Moreira, A.F.; de Melo-Diogo, D.; Gaspar, V.M.; Carvalho, M.P.; Correia, I.J. 3D tumor spheroids: An overview on the tools and techniques used for their analysis. *Biotechnol. Adv.* **2016**, *34*, 1427–1441. [[CrossRef](#)]
48. Friedl, P.; Alexander, S. Cancer invasion and the microenvironment: Plasticity and reciprocity. *Cell* **2011**, *147*, 992–1009. [[CrossRef](#)]
49. Yamada, M.; Sekiguchi, K. Molecular Basis of Laminin-Integrin Interactions. *Curr. Top. Membr.* **2015**, *76*, 197–229.
50. Rognoni, E.; Ruppert, R.; Fässler, R. The kindlin family: Functions, signaling properties and implications for human disease. *J. Cell. Sci.* **2016**, *129*, 17–27. [[CrossRef](#)]

51. Yamaguchi, H.; Condeelis, J. Regulation of the actin cytoskeleton in cancer cell migration and invasion. *Biochim. Biophys. Acta* **2007**, *1773*, 642–652. [[CrossRef](#)]
52. Tolar, P. Cytoskeletal control of B cell responses to antigens. *Nat. Rev. Immunol.* **2017**, *17*, 621–634. [[CrossRef](#)] [[PubMed](#)]
53. Han, D.; Moon, S.; Kim, Y.; Kim, J.; Jin, J.; Kim, Y. In-depth proteomic analysis of mouse microglia using a combination of FASP and StageTip-based, high pH, reversed-phase fractionation. *Proteomics* **2013**, *13*, 2984–2988. [[CrossRef](#)] [[PubMed](#)]
54. Rappsilber, J.; Mann, M.; Ishihama, Y. Protocol for micro-purification, enrichment, pre-fractionation and storage of peptides for proteomics using StageTips. *Nat. Protoc.* **2007**, *2*, 1896–1906. [[CrossRef](#)] [[PubMed](#)]
55. Han, D.; Jin, J.; Woo, J.; Min, H.; Kim, Y. Proteomic analysis of mouse astrocytes and their secretome by a combination of FASP and StageTip-based, high pH, reversed-phase fractionation. *Proteomics* **2014**, *14*, 1604–1609. [[CrossRef](#)]
56. Tyanova, S.; Temu, T.; Cox, J. The MaxQuant computational platform for mass spectrometry-based shotgun proteomics. *Nat. Protoc.* **2016**, *11*, 2301–2319. [[CrossRef](#)]
57. Cox, J.; Neuhauser, N.; Michalski, A.; Scheltema, R.A.; Olsen, J.V.; Mann, M. Andromeda: A peptide search engine integrated into the MaxQuant environment. *J. Proteome Res.* **2011**, *10*, 1794–1805. [[CrossRef](#)]
58. Kim, J.Y.; Lee, H.; Woo, J.; Yue, W.; Kim, K.; Choi, S.; Jang, J.J.; Kim, Y.; Park, I.A.; Han, D.; et al. Reconstruction of pathway modification induced by nicotinamide using multi-omic network analyses in triple negative breast cancer. *Sci. Rep.* **2017**, *7*, 3466. [[CrossRef](#)]
59. Carey, S.P.; Martin, K.E.; Reinhart-King, C.A. Three-dimensional collagen matrix induces a mechanosensitive invasive epithelial phenotype. *Sci. Rep.* **2017**, *7*, 42088. [[CrossRef](#)]
60. Detre, S.; Saclani Jotti, G.; Dowsett, M. A “quickscore” method for immunohistochemical semiquantitation: Validation for oestrogen receptor in breast carcinomas. *J. Clin. Pathol.* **1995**, *48*, 876–878. [[CrossRef](#)]
61. Vizcaíno, J.A.; Deutsch, E.W.; Wang, R.; Csordas, A.; Reisinger, F.; Ríos, D.; Dienes, J.A.; Sun, Z.; Farrah, T.; Bandeira, N.; et al. ProteomeXchange provides globally coordinated proteomics data submission and dissemination. *Nat. Biotechnol.* **2014**, *32*, 223–226. [[CrossRef](#)]
62. Kaimal, V.; Bardes, E.E.; Tabar, S.C.; Jegga, A.G.; Aronow, B.J. ToppCluster: A multiple gene list feature analyzer for comparative enrichment clustering and network-based dissection of biological systems. *Nucleic Acids Res.* **2010**, *38*, W96–W102. [[CrossRef](#)] [[PubMed](#)]
63. Szklarczyk, D.; Gable, A.L.; Lyon, D.; Junge, A.; Wyder, S.; Huerta-Cepas, J.; Simonovic, M.; Doncheva, N.T.; Morris, J.H.; Bork, P.; et al. STRING v11: Protein-protein association networks with increased coverage, supporting functional discovery in genome-wide experimental datasets. *Nucleic Acids Res.* **2019**, *47*, D607–D613. [[CrossRef](#)] [[PubMed](#)]
64. Shannon, P.; Markiel, A.; Ozier, O.; Baliga, N.S.; Wang, J.T.; Ramage, D.; Amin, N.; Schwikowski, B.; Ideker, T. Cytoscape: A software environment for integrated models of biomolecular interaction networks. *Genome Res.* **2003**, *13*, 2498–2504. [[CrossRef](#)] [[PubMed](#)]
65. Tyanova, S.; Temu, T.; Sinitcyn, P.; Carlson, A.; Hein, M.Y.; Geiger, T.; Mann, M.; Cox, J. The Perseus computational platform for comprehensive analysis of (prote)omics data. *Nat. Methods* **2016**, *13*, 731–740. [[CrossRef](#)] [[PubMed](#)]

